EMAP5: A 3D HYBRID FEM/MoM CODE

Yun Ji and Todd H. Hubing
University of Missouri-Rolla

Abstract--EMAP5 is a numerical software package designed to model electromagnetic problems. It employs the finite element method (FEM) to analyze a volume, and employs the method of moments (MoM) to analyze the current distribution on the surface of the volume. The two methods are coupled through the electric fields on the dielectric surface. The filed behavior at dielectric/metal junctions is modeled by three-way basis functions. EMAP5 can model three kinds of source: incident plane wave, voltage sources on metal patches and impressed current sources in the finite element region. Three numerical examples are provided to demonstrate the validity of the code.

I.   FORMULATION

Although details of EMAP5 formulation are provided in [1][2], a brief summary is provided below. The general structure of interest is shown in Figure 1. A dielectric volume V_2 has electrical properties (ε_2, μ_2). It is enclosed by a surface S_2. A conductive volume V_3 is enclosed by a conductive surface S_c. The fields within V_3 vanish. V_1 denotes the volume outside of V_2 and V_3, and has electrical properties (ε_1, μ_1). V_1 is assumed to be free space. (E_1, H_1) and (E_2, H_2) denote the electric and magnetic fields in V_1 and V_2, respectively. The unit normal vectors for S_2 and S_c are defined pointing outward toward V_1. The structure is excited by an incident wave (E^i, H^i) or impressed sources (J^{int}, M^{int}). The scattered electric and magnetic fields are (E^s, H^s). The objective is to solve for the scattered fields (E^s, H^s) or the surface electric current density on S_c.

1. <u>Discretization of FEM</u>   From Maxwell equations, the double curl equation in terms of E can written:

$$\nabla \times \left(\frac{1}{j\omega\mu_0\mu_r} \nabla \times E(r) \right) + j\omega\varepsilon_0\varepsilon_r E(r) = -J^{int}(r) - \frac{1}{j\omega\mu_0\mu_r} \nabla \times M^{int}(r) \tag{1}$$

After multiplying Eq. (1) by a weighting function $w(r)$ and integrating over the finite element domain V_2, one obtains the FEM weak form as follows:

$$\int_{V2} \left[\left(\frac{1}{j\omega\mu_0\mu_r} \nabla \times E(r) \right) \bullet (\nabla \times w(r)) + j\omega\varepsilon_0\varepsilon_r E(r) \bullet w(r) \right] dV = \int_{S2} (\hat{n} \times H(r)) \bullet w(r) \, dS$$

$$- \int_{V2} \left[J^{int}(r) + \frac{1}{j\omega\mu_0\mu_r} \nabla \times M^{int}(r) \right] \bullet w(r) \, dV \tag{2}$$

Tetrahedral elements are used to discretize the volume V_2. Basis and weighting functions proposed by M. L. Barton and Z. J. Cendes [3] are chosen here. Each basis function is defined within a tetrahedron and is associated with one of the six edges. The electric field E within volume V_2 can be expanded as:
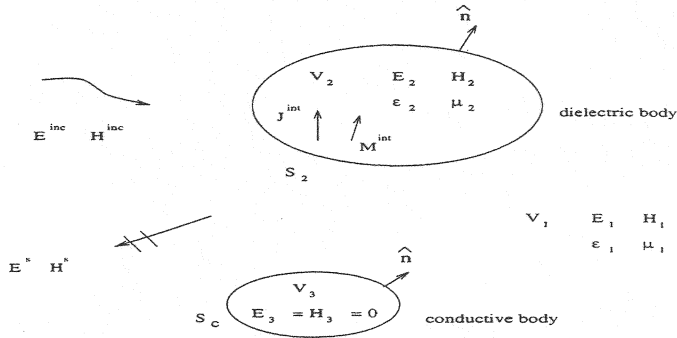
928

Fig. 1. A dielectric obect and a conductive object illuminated by E^i, H^i or J^{int}, M^{int}.

$$E(r) = \sum_{n=1}^{N_v} E_n \, w_n(r)$$

where N_v is the total number of interior edges, and $\{E_n\}$ is a set of unknown complex scalar coefficients.

The surface integral term in Eq. (2) can be evaluated by using a surface basis function $f(r)$, which are discussed later. Using a Galerkin's approach, a discrete form of Eq. (2) is obtained:

$$\begin{bmatrix} A_{ii} & A_{id} \\ A_{di} & A_{dd} \end{bmatrix} \begin{bmatrix} E_i \\ E_d \end{bmatrix} = \begin{bmatrix} 0 & 0 \\ 0 & B_{dd} \end{bmatrix} \begin{bmatrix} 0 \\ J_d \end{bmatrix} + \begin{bmatrix} 0 \\ g \end{bmatrix} \tag{3}$$

where $[J_d]$ is a set of unknown complex scalar coefficients for the surface electric current densities on S_d. S_d is defined as S_2 if the conductive body is not adjacent to the dielectric body; Otherwise, $S_d = S_2 - (S_2 \cap S_c)$. The unknown coefficients $[E]$ are partitioned according to edge type. The two categories are interior edges, which are denoted by a subscript i in Eq. (3), and dielectric boundary edges, which are denoted by a subscript d in Eq. (3). $[g^{int}]$ is the forcing term. Details of how to evaluate the elements of $[A]$, $[B]$ and $[g^{int}]$ are provided in [1][2].

2. Discretization of MoM   The MoM surface integral equation is [4]:

$$E^{inc}(r) = \frac{1}{2} E(r) + \int_S \{ M(r') \times \nabla' G_0(r, r') + j k_0 \eta_0 J(r') G_0(r, r') - j \frac{\eta_0}{k_0} \nabla' \bullet J(r') \nabla G_0(r, r') \} dS' \tag{4}$$

where $r \in S$, $S = S_c \cup S_2$, η_0 and k_0 are the intrinsic impedance and wavenumber in free space, respectively, and

$$G_0(r, r') = \frac{e^{-j k_0 |r - r'|}}{-4\pi |r - r'|}$$

is the Green's function in free space. The surface equivalent electric and magnetic currents are defined as:

$$\mathbf{J}(\mathbf{r}') = \hat{n} \times \mathbf{H}(\mathbf{r}') \qquad \mathbf{r}' \text{ on S}; \qquad \mathbf{M}(\mathbf{r}') = \mathbf{E}(\mathbf{r}') \times \hat{n} \qquad \mathbf{r}' \text{ on } S_d.$$

$\mathbf{M}(\mathbf{r}')$ vanishes on S_c. $\mathbf{J}(\mathbf{r}')$ and $\mathbf{M}(\mathbf{r}')$ can be approximated by using the triangular basis function $\mathbf{f}_n(\mathbf{r})$ proposed by S. M. Rao *et al.* [5].

On surface S_d, the MoM basis function $\mathbf{f}_n(\mathbf{r})$ and the FEM basis function $\mathbf{w}_n(\mathbf{r})$ are related by:

$$\mathbf{w}_n(\mathbf{r}) = \hat{n} \times \mathbf{f}_n(\mathbf{r}) \qquad \mathbf{r} \in S_d$$

$\mathbf{J}(\mathbf{r}')$, $\mathbf{M}(\mathbf{r}')$ can be expanded as:

$$\mathbf{J}(\mathbf{r}') = \hat{n} \times \mathbf{H}(\mathbf{r}') = \sum_{n=1}^{N_s} J_n \mathbf{f}_n(\mathbf{r}') \qquad \mathbf{M}(\mathbf{r}') = \mathbf{E}(\mathbf{r}') \times \hat{n} = \sum_{n=1}^{N_d} E_n \mathbf{f}_n(\mathbf{r}')$$

where N_s is the total number of edges on the surface S, and N_d is the total number of edges on the surface S_d. $\{J_n\}$ and $\{E_n\}$ are unknown complex scalar coefficients.

The weighting functions chosen are $\mathbf{f}_n(\mathbf{r})$, n=1, ... N_s. After $\mathbf{f}_n(\mathbf{r})$ are multiplied to Eq. (4), Eq. (4) can be discretized into Eq. (5), which is a matrix equation. Edges on S_d and S_c are grouped together respectively.

$$\begin{bmatrix} C_{dd} & C_{dc} \\ C_{cd} & C_{dd} \end{bmatrix} \begin{bmatrix} J_d \\ J_c \end{bmatrix} = \begin{bmatrix} D_{dd} & 0 \\ D_{cd} & 0 \end{bmatrix} \begin{bmatrix} E_d \\ 0 \end{bmatrix} - \begin{bmatrix} F_d^i \\ F_c^i \end{bmatrix} \qquad (5)$$

$[F^i]$ is the forcing term due to the incident wave. A description of how to evaluate the elements of $[C]$, $[D]$ and $[F^i]$ are is provided in [1][2]. $[J_c]$, $[J_d]$, $[E_i]$, $[E_d]$ can be solved from Eq. (3) and Eq. (5).

II.   COMPONENTS OF THE EMAP5 SOFTWARE PACKAGE

The EMAP5 software package includes three major components: SIFT5, EMAP5 and FAR.

1. <u>SIFT5: The Input File Translator</u>   Standard Input File Translator Version5 (SIFT5) is designed to generate input files for the field solver EMAP5. SIFT5 reads a text file in the SIFT format [5]. Users can describe the structure of interest by using eleven keywords shown in Table I. The physical geometry, source, and the output requirements must be specified.
    The input file for SIFT5 should have a .sif suffix. The output file of SIFT5 has a .in suffix. For example, if a user has composed an input file E1.hbs, the following command will generate an input file E1.in for EMAP5.
    % sift5 E1.sif

2. <u>EMAP5: The FEM/MoM Field Solver</u>   EMAP5 is the hybrid FEM/MoM field solver. It reads a file generated by SIFT5. The input file should have a .in suffix. A file with a .log suffix is generated to log running status and error messages. EMAP5 will print fields within areas specified by the keyword "output", to one or more output files. All equivalent surface currents $\mathbf{J}$ and $\mathbf{M}$ will be printed out by using the keyword "default_out". An example of how to run EMAP5 follows:
    % emap5 E1.in
    EMAP5 will read the mesh file E1.in as its input. In addition, E1.log will be generated immediately as the log file.

3. <u>FAR: The Far Field Calculator</u>   FAR is a program used to calculate the far field radiation pattern. The far fields are calculated from the equivalent surface currents $\mathbf{J}$ and $\mathbf{M}$. FAR needs two input files. One is the file generated by SIFT5, and the other is the default output file generated by

Table I. Syntax of keywords for SIFT5.

keyword	position coordinates	cell dimensions	sub attributes
#			
unit			number in m, cm or mm
boundary	x1 y1 z1 x2 y2 z2		
celldim	p1, p2	Δp	axis (x, y or z)
dielectric	x1 y1 z1 x2 y2 z2		ε' ε'' (The real and imaginary part of the complex permittivity)
conductor	x1 y1 z1 x2 y2 z2	Δx Δy Δz	
eplane			frequency,$\theta 1$, $\varphi 1$, $\theta 2$, $\varphi 2$, magnitude,
vsource	x1 y1 z1 x2 y2 z2		frequency, polarization (x, y, z), magnitude,
isource	x1 y1 z1 x2 y2 z2		frequency, polarization (x, y, z), magnitude,
output	x1 y1 z1 x2 y2 z2		axis(x, y, z) filename
default_out			filename

EMAP5. Assuming the default output file of EMAP5 is E1.out, and the input file is E1.in, the following command will run the far field calculator.

% far E1.in E1.out far.out

where far.out is the file to which the far field will be printed when the program terminates. The far.out file will contain an array of (θ, φ, E_θ, E_φ) data. E_θ and E_φ, whose units are volts/meter, are the E fields at point (R, θ, φ) in spherical coordinates.

III. NUMERICAL RESULTS

The first configuration is a flat dipole antenna in free space. Although EMAP5 is a FEM/MoM code, it can model configurations that require only one method to analyze. In this case, only the MoM portion of the code is employed. As shown in Figure 2, a center-fed flat dipole has a width of one millimeter and a length of 44 centimeters. It is fed by a 300-MHz voltage source with a magnitude of one volt. The input file for SIFT5 is as follows:

 # example 1: a flat dipole antenna driven by a voltage source in the middle
unit 0.5 mm
conductor   0   0 2 880   2   2   10 1   1
vsource   440   0 2 440   2   2   300 x 1.0

931

output   0 0 2 840   2 2   y example1.out

The structure is divided into 268 triangles. The total number of unknown edges is 438. The output of EMAP5 is the surface electric current J along the flat dipole. The current at the source is given by:

$$I = J_f * w$$

where J_f is a complex number denoting the surface current across the source edge, and w is the width of the edge. In this example, two edges are used to model the source. Thus, the total current is the sum of currents across the two edges. The input impedance of the dipole is given by:

$$Z_{in} = \frac{1.0 \text{ v}}{I}$$

Figure 3 shows the input resistance, input reactance and impedance obtained by EMAP5 as the dipole length is adjusted from 38-53 cm, with a comparison of analytical results by treating the flat dipole as a cylindrical dipole with an equivalent radius[6]. Good agreement between EMAP5 and theoretical results is achieved.

The second configuration, as shown in Figure 4, is a flat dipole consisting of two quarter-wavelength traces driven by a 533-MHz voltage source with a magnitude of one volt. In this case, the source is located within the FEM region. Since the width of the traces is very small compared with the width of the FEM region, a non-uniform mesh is used to discretize the structure. Near the junction and source areas, small cells are used. Initially, the relative permittivity of the dielectric slab is set to 1.0. Thus, the configuration is a half-wave dipole in free space. The source is modeled as a current filament that coincides with two tetrahedron edges. After the E fields along these two edges are obtained, the voltage drop along the current filament can be calculated. The input file for SIFT5 is as follows,

 # example 2: a dipole driven by a current source located within the FEM region
unit 0.25 mm
boundary   0   0   0   164 82 2
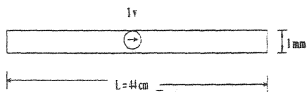*celldim   0   2   2   x*
celldim   2   162 16   x

Fig. 2. A flat dipole with a width
width of 1 mm.

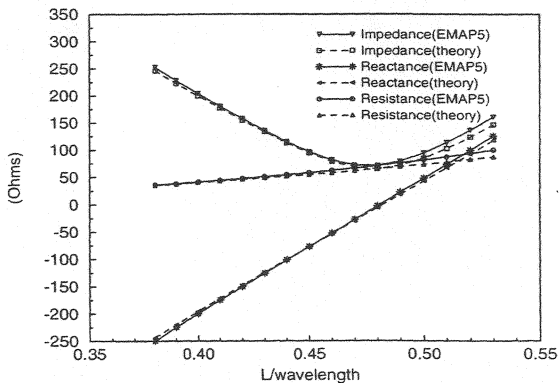Fig. 3. Input impedance of a flat dipole length of 44 cm and a
antenna with L=38~53 cm, width = 1 mm.
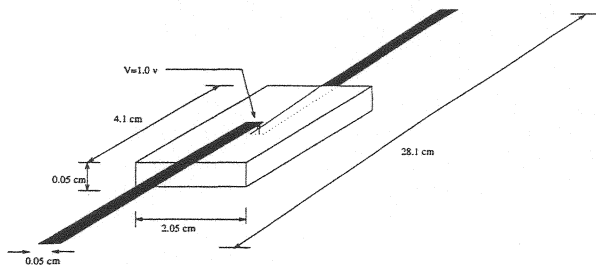
Fig. 4. Geometry of a PCB antenna.

```
celldim     162 164  2    x
celldim     0    40  10   y
celldim     40   42  1    y
celldim     42   82  10   y
celldim     0    2   1    z
dielectric  0    0   0    164  82  2   1.0  0.0
conductor  -480  40  2    82   42  2   10  1  1
conductor   82   40  0    644  42  0   10  1  1
isource     82   41  0    82   41  2   533 z  1
output     -480  40  2    0    42  2   y   example2.out
output      164  40  0    644  42  0   y   example2.out
```

The FEM region is divided into 1200 tetrahedra. The boundary is divided into 2632 edges. The number of unknown edges for the final matrix equation is 1900. The current distribution on the traces obtained using EMAP5 is plotted in Figure 5. For comparison, the results obtained using the Numerical Electromagnetics Code (NEC) and the IBM EM Simulator are also plotted. Figure 6 shows the results obtained by EMAP5 and the IBM EM Simulator when the dielectric constant is set to 10.0. In both cases, the results obtained using the different methods are similar.

The third configuration shown in Figure 7 is a dielectric cube with 0.2λ on a side, where λ is the wavelength in free space. It is illuminated by an incident wave, which travels along the +z axis. The E field is polarized along the x axis with a magnitude of one volt/meter. This example has been previously analyzed by T. K. Sarkar et al.[7], B. J. Rubin and S. Dajiavad [8]. First, the dielectric constant of the cube is set to 1-j1000. The input file for SIFT5 is as follows,

```
# example 3: a dielectric cube (εr =1-j1000 ) illuminated by a plane wave
unit      1  mm
boundary    -50  -50  -50 50  50  50
celldim     -50   50   25  x
celldim     -50   50   25  y
celldim     -50   50   25  z
dielectric  -50  -50  -50 50  50  50  1.0  -1000.0
eplane   600  90   0  0   0  1.0
default_out   example3.out
```

933

The dielectric cube is divided into 64 bricks, then 320 tetrahedra. In Figure 8, the normalized far field obtained by EMAP5 is compared to those calculated in [7][8]. Second, the dielectric constant of the cube is set to 9.0. The "dielectric" line in the input file for SIFT5 need to be changed as follows,

dielectric -50 -50 -50 50 50 50 9.0 0.0

In Figure 9, the normalized far field obtained by EMAP5 is compared to those calculated in [7] [8]. In both cases, the results obtains by EMAP5 agrees with the references.
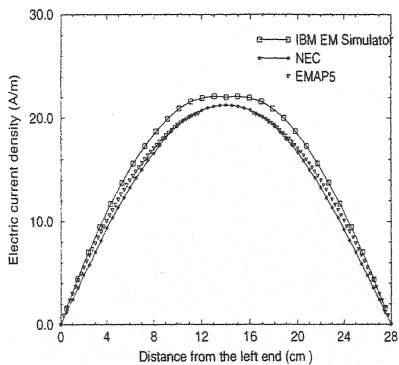
Fig. 5. Current distribution
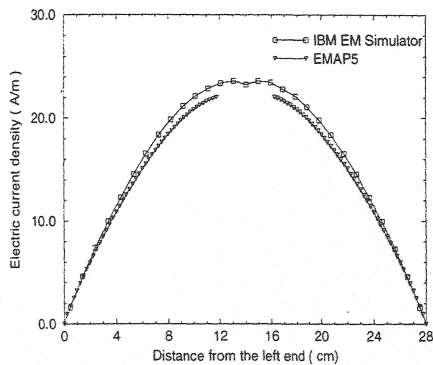on the dipole(ε_r=1.0).

Fig. 6. Current distribution
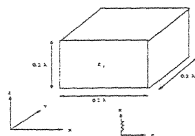on the dipole (ε_r=10.0).

Fig. 7. A dielectric cube
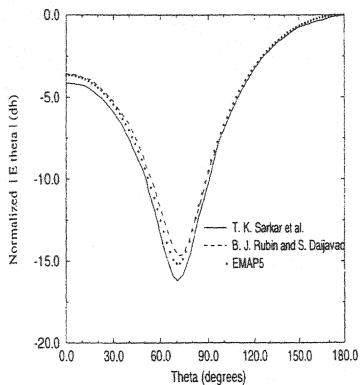illuminated by a plane wave

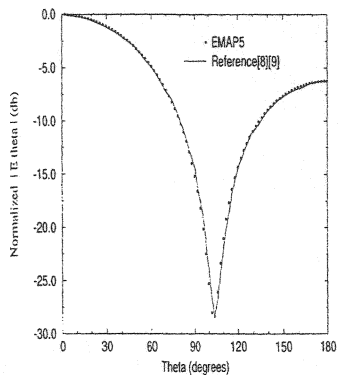Fig. 8. Comparison of far field
Eθ when ε_r = 1-j1000.

Fig. 9. Comparison of far field
Eθ when ε_r =9.

934

Reference:

[1]   M. W. Ali, T. H. Hubing and J. L. Drewniak, "A Hybrid FEM/MoM Technique for Electromagnetic Scattering and Radiation from Dielectric Objects with Attached Wires," *IEEE Trans. on Electromagnetic Compatibility*, vol. 39, pp. 304-314, November 1997.

[2]   Mohammad W. Ali, "Development of a Hybrid 3D numerical Modeling Technique for Analyzing Printed Circuit Models with Attached Wires," Ph.D. dissertation, University of Missouri-Rolla, December 1996.

[3]   M. L. Barton and Z. J. Cendes, "New Vector Finite Elements for Three-Dimensional Magnetic Field Computation," *Journal of Applied Physics*, vol. 61, pp. 3919-3921, April 1982.

[4]   Johnson J. H. Wang, *Generalized Moment of Methods in Electromagnetics*, New York: John Wiley & Sons, 1990.

[5]   S. M. Rao, D. R. Wilton, and A. W. Glisson, "Electromagnetic Scattering by Surfaces of Arbitrary Shape," *IEEE Trans. on Antennas and Propagat.*, vol. 30, pp. 409-418, May 1982.

[6]   T. H. Hubing, C. Hong-Him Lim and J. Drewniak, "A Geometry Description Language for 3D Electromagnetic Analysis Codes," *Proceedings of the 10th Annual Review of Progress in Applied Computational Electromagnetics*, pp. 417-422, March 1994.

[7]   Constantine A. Balanis, *Antenna Theory Analysis and Design*, 2nd Edition, New York: John Wiley & Sons Inc, 1997.

[8]   T. K. Sarkar, E. Arvas, and S. Ponnapalli, "Electromagnetic Scattering from Dielectric Bodies," *IEEE Trans. Antenna Propagat.*, vol 32, pp. 77-85, Jan. 1984.

[9]   B. J. Rubin and S. Daijavad, "Radiation and Scattering from Structures Involving Finite-Size Dielectric Regions", *IEEE Trans. Antenna Propagat.*, vol 38, pp. 1863-1873, Nov., 1990.